IOSR Journal of Mechanical and Civil Engineering (IOSR-JMCE)
e-ISSN: 2278-1684,p-ISSN: 2320-334X, Volume 16, Issue 3 Ser. III (May. - June. 2019), PP 50-66
www.iosrjournals.org

A Novel Proposal of Partial Fixation Joints to Raise the Load Carrying Capacity of Existing Ribbon Type Floating Bridges

Hisham A. El-Arabaty[1]
[1]*Associate Professor, Structural Engineering Department, Faculty of Engineering, Ain-Shams University, Cairo, Egypt.*
Corresponding Author: Hisham A. El-Arabaty

Abstract: *The objective of this research work is to study the structural behavior of "ribbon-type" floating bridges, and the effect of the type of joints connecting the pontoons on the "load – carrying" capacity of these floating bridges.The research presented here is mainly directed towards investigation of a newly proposed partial fixation joint, formed by rubber bumpers separated by a gap at the top of the pontoons, acting in conjunction to the standard steel hinge at the pontoons bottom.*
The analytical model and software package developed in a previous research work is extended to include the newly proposed partial-fixation joint.
Emphasis is placed on the study of existing under-strength ribbon bridges of the "hinged-type" connection, with an extensive parametric study directed at investigating the possibility of using this new type of joint to raise the load-carrying capacity of the bridges, reducing their vertical deflection into the water during the passage of heavy vehicles, while at the same time minimizing the additional moments incurred in the process.
The results of the study are used to develop design tables and figures to aid designers in selecting a suitable configuration for "partial-fixation" joints to strengthen existing pontoon bridges. Important conclusions and recommendations are presented related to the practical use of the proposed joint.
Keywords: *Floating Bridges, Partial-Fixation Joint, Bridge Strengthening, Stiffness Method, Virtual Work Method.*

Date of Submission: 20-05-2019 Date of acceptance: 05-06-2019

I. Introduction

While floating bridges exist in several types and shapes, the "ribbon-type" pontoon bridge is a very special type of bridge, characterized by its high speed of erection, and its ability to bridge the gap imposed by a large waterway.The recent increases in vehicle weights have rendered many existing pontoon bridges incapable of carrying these new vehicles, as the flotation volume of the pontoons produces insufficient water upthrust forces to carry the imposed vertical loads.

This study deals with a novel proposal for a new type of joint, connecting the pontoons together, which serves to modify the pontoon behavior from the standard "hinged-connection" bridge to a "partial-fixation-connection" bridge, thus raising its load carrying capacity to meet current loading conditions, while at the same time, avoiding the tremendous increase in moments produced by a "fully-fixed-connection" between pontoons of the floating ribbon bridge.

II. Existing Literature And Pontoon Description

A typical pontoon bridge is composed of a number of interior bays, 2 ramp bays at the start and end of the bridge. The pontoons are carried to the waterway location using special trucks, unloaded into the water, and assembled to form the bridge. Figure 1 shows a photo of a typical pontoon unit after being dropped into the water. As seen, the folded pontoon unit unfolds as it touches the water, by virtue of springs. Once the shown 4 segments are fixed in place using joints and latches, the pontoon unit is ready to be assembled into its place in the overall bridge structure.

Figure 1. Single Pontoon unfolding into water

The pontoon units are assembled together to form the bridge body as shown in the photo in figure 2. Special boats are used to stabilize the bridge in the transverse direction, in order to counter the effect of the transverse forces exerted by the water currents. In the vertical direction, the pontoon bridge relies on upward buoyancy forces to counter the vertical loads imposed by the bridge weight and the effect of the passing vehicles. Its structural behavior in the vertical direction is similar to a beam on elastic foundations.

Figure 2. Photo of Pontoon bridge after installation over waterway

Several research studies were directed to the study of the pontoon ribbon bridge behavior, with emphasis on its buoyancy, its static and dynamic response to moving loads, and on the pontoons' design and strength.Severalresearch studies conducted in this field focused on practical problems encountered during the installation and use of existing pontoon bridges.

Wael M. Al-Badrawy (2002) developed an interactive dynamic analysis algorithm, utilizing a sophisticated vehicle model together with the bridge model. Sub-structuring and Matrix condensation were used to take into consideration the continuous change in model geometry as the vehicle passes from one point to another on the bridge. The axle and tyre stiffnesses were included in the model, and the developed algorithm was used for the analysis of existing roadway bridges.

Shixiao Fu, Weicheng Cui, Xujun Chen and Cong Wang, (2005), used the finite element method to model floating bridges with nonlinear connectors. Hydrostatic analysis of the bridge was performed taking into consideration the existing nonlinearity, and the presence of "initial gap" in the connectors. The work by **Shixiao Fu, Torgeir Moan, Xujun Chen and Weicheng Cui, (2007)**, focused on a two-module interconnected model,

capable of predicting the resulting displacments and straining actions of the interconnected structures. Effect of the module stiffness and the connector on the hydro-elastic response are studied, with the purpose of reaching optimal design of the structure.

The concept of joining 2 or 3 pontoons together through fixed joints to form Double & Triple Pontoon Units was investigated by **Ehab M. Ebeid (2006)**. Dynamic analysis of the bridge/vehicle/fluid system was performed to determine the effect of using these proposed units. The Use of double and triple pontoon units was found to enhance the bridge performance considerably reducing the overall displacement, and increasing its load carrying capacity. However, a consequence of this upgrade was found to be the sharp increase in bending moments developed in the bridge body, and at the fixed joints. This effect was more pronounced for the triple pontoon units.

The work by **Hisham A. El-Arabaty (2007)**, focused on the effect of the transverse loading imposed by the waterway currents on the bridge body. Detailed analysis of pontoon bridges in the transverse direction was performed, with an emphasis on assessment of the effect of the reaction forces produced by the supporting boats on the straining actions in the bridge body in the transverse direction. Proposals were made for reducing the level of straining actions and the sensitivity of the bridge to the up/down variations of both bridge movements and boat reactions.

Mitra S. and SinhamahapatraK.P., (2008),utilized linear structural elements, in combination with 2-D fluid elements for the finite element analysis of the combined fluid-structure system. The pressure variable ws used to express the fluid system. An iterative procedure was used to simulate the fluid structure interaction. The author used the Galerkin weighted residual method, and the results were compared with existing cases.

A research study was conducted by **Wael M. Al-Badrawy (2009)**for the dynamic analysis of existing pontoon bridges under the effect of multiple vehicles passing on the bridge. A previously developed software was updated to include the multiple vehicle models, and a parametric study was performed with an emphasis on the assessment of the effect of the distance left between consecutive vehicles, on the pontoon bridge behavior. In addition, the effect of the vehicles' weight and speed was also studied in detail.

In **Nasr E. Nasr (2009)**, the torsional stability of the bridge during the passage of vehicles on it was studied in detail. An analytical algorithm was developed together with a software package to determine the nonlinear variation of the torsional stabilizing effect exerted by water upthrust forces. The exact shape of the pontoon body including the curvature of the bow segments was considered, and important conclusions were developed related to the causes of frequent torsional instability of some bridges.

The effect of a moving two-axle vehicle on the behavior of ribbon bridges was investigated both experimentally and analytically by **Giannin Viecili (2014).** This research focused on the assessment of the optimum transportability of vehicles and supplies across floating bridges. In order to allow more traffic to pass the bridge more rapidly, recommendations were reached based on the study results. A main recommendation is the enlargement of pontoon size. The study also focused on the effect of both the speed and weight of the passing vehicles.

Qayed R. Eid (2016), research focused on the strengthening of existing pontoon bridges, and the upgrade of their load carrying capacity. Detailed dynamic analysis of typical pontoon bridges was conducted on a wide range of vehicle loads, passing the bridge at varying speeds. The damping effect of the fluid added mass was studied in detail, and a proposal was made for development of a partial fixation joint without rubber bumpers. A wide variety of dynamic analysis runs were used to establish the expected range of dynamic amplification factors for both bridge maximum displacement and bending moment values.

III. Problem Description

The types of joints connecting ribbon bridge pontoons can be generally classified into 2 types, mainly hinged and fixed joints. The hinged joints are more common in older existing models of these bridges, as the pontoons are joined by a hinge at their lower end only. This behavior is illustrated in Figure 3.

Some newer models utilize the fixed type joints, where the pontoons are connected together on site at top and bottom, thus forming a compression/tension couple which constitutes a fixation moment between the pontoons. This type of fixation serves to modify the bridge's structural behavior from that of a group of small spans (pontoons) connected through hinges, to a large span comprising several pontoons connected together.

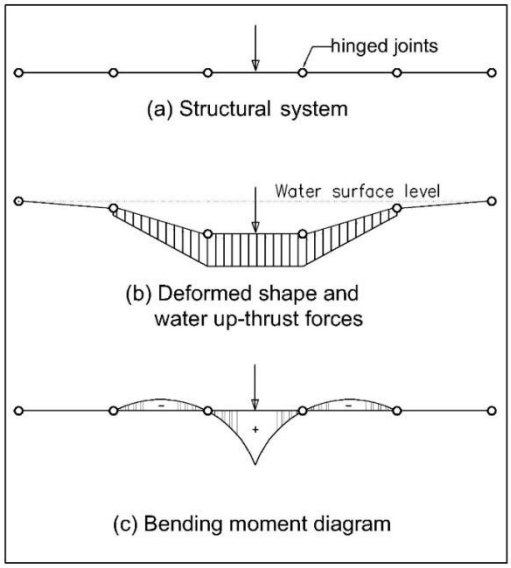

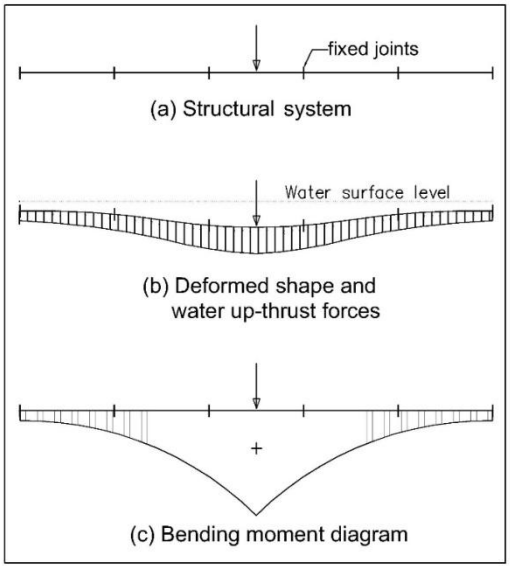

As shown in Figure 4, this fixation moment reduces the bridge's displacement considerably, and thus enables it to carry high loads, without the risk of being submerged excessively under water. On the other hand, this enlarged bridge connected span acts as a double cantilever beam carrying a load at its middle.

In order to utilize the fixed joints in a bridge therefore requires design of new pontoons, and joints which can withstand the expected high level of straining actions associated with it. Adding fixed joints to existing pontoons originally designed as hinged joint pontoons would produce very high values of bending moments, and would thus render the current configuration of the existing bridge pontoons unsafe.

The approach taken in this paper is directed to the development of a partial-fixation joint which would raise the load-carrying capacity of existing ribbon bridges in a sufficient manner so as to reduce bridge deflection, and allow passage of current vehicles, while producing a minimum effect on the expected increase of bending moments and straining actions in the bridge body, so as to allow for use of the existing pontoons without a need for drastic modifications or replacement.

The joint proposed in this research is composed of rubber bumpers at the top of the pontoons, which leave a limited gap between them. The standard steel joint at the bottom acts together with the bumpers to produce fixation effect but only after a certain deformation has been achieved, and therefore the "partial fixation" effect is produced. Analysis results under effect of expected vehicle loads, utilizing different configurations of gap distance, and bumper thickness can give the designer the flexibility of deciding which level of fixation is sufficient, and at the same time makes it possible to minimize the unwanted effect of increased straining actions in the bridge body and joints.

IV. Proposed Partial Fixation Rubber-Bumpers Joint

The main concept of the newly proposed joint is to exhibit an intermediate structural behavior between the existing "Totally hinged" joint, and a "Fully fixed" joint. In the existing bridges selected for this study, a hinged joint near the lower edge of the pontoons serves to connect the pontoons together while allowing free rotation between the pontoons. This results in the top points of the adjacent pontoons coming nearer to each other when vehicles are passing on bridge top, thus reducing the gap distance between them.

The use of these hinged joints produces high vertical displacement of the individual pontoons, and it is very common to see the loaded spans dive deeply into the water as the vehicles pass upon them, as illustrated in figure 3. With the current increase in vehicle weights, this deep dive into water can reach the point where the whole pontoon is under water, and the flotation forces are not sufficient to keep the pontoons and vehicles afloat. Replacing these joints with "fully fixed" joints would definitely overcome the above problem, and reduce the bridge's downward displacement greatly. This is caused by the fact that several spans act together to carry the vehicle loads, and thus the resulting displacements are reduced significantly. However, this change in behavior would produce much higher moments, as the cantilever arm of the acting bridge body extends far longer, as explained in detail in section 3, and illustrated in figure 4.

The new approach proposed in this study is based on achieving "partial-fixation" at the joints connecting the pontoons. This partial fixation is sufficient to keep the bridge afloat under the expected loads, while minimizing the undesirable side effect of increased straining actions in the bridge body.

4.1. Joint configuration and basic behavior

The newly proposed joints are based on keeping the existing joints at the bottom of the pontoons, while adding rubber bumpers of specified widths to fill part of the gap between the top points. Figure 5 shows the proposed joint configuration, and the expected movement of the pontoons. As the loaded pontoon moves downward, the gap between the top rubber bumpers is reduced in size, while allowing a limited rotation angle to occur between the pontoons, as shown in figure 5a.

Once the bumpers touch each other, the joint is closed at the top (see figure 5b). As the joint rotation increases beyond this point, The bumpers start to produce a compression force at the top, which forms a couple with the tension force in the bottom joint, thus producing bending moments which are transferred to the adjacent pontoonsand the rate of rotation is significantly reduced (see figure 5c). This development of "partial fixation" at the joint serves to increase the overall bridge stiffness, and to increase the contribution of the adjacent pontoons in carrying the vehicle loads with the loaded pontoon, thus reducing the expected displacement downward into the water, and allows the bridge to carry the higher vehicle loads, without being totally submerged into the water.

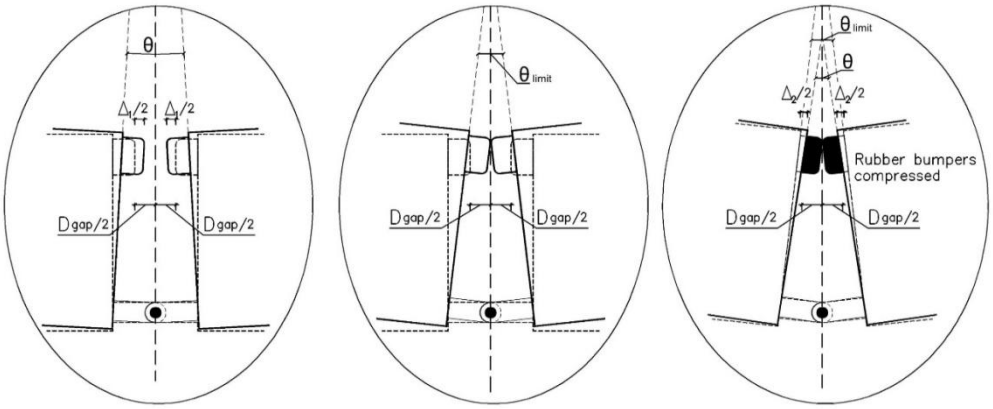

a. Hinged joint Rotation b. Bumpers touch each other c. Compressed Bumpers develop fixation moment

Figure 5. Movement patterns of the proposed partial-fixation joint

The different stages of the joint behavior are illustrated in figure 5 above, where the proposed joint is shown in both the open (hinged) and shut (fixed) cases. Figure 5a shows the "hinged-joint" action, as the rotation is still small enough to keep the bumpers apart. This behavior dominates as long as the pontoons are not yet loaded enough to exhibit high rotation values in the joints ($\theta < \theta_{limit}$). In figure 5b, a critical point is reached, where sufficient rotation has occurred so that the 2 bumpers touch each other but no deformation occurs yet in the bumpers ($\theta = \theta_{limit}$). Figure 5c illustrates the last stage of behavior, where additional movement of the pontoons produces an increase in the joint rotation ($\theta > \theta_{limit}$). The bumpers are compressed, and the joint consequently exhibits a fixed-joint behavior, and a bending moment starts to develop at the joint between the pontoons.

4.2. Computation of the joint rotational stiffness

As the joint rotates in a direction reducing the gap distance, a rotation angle (θ) develops as shown in figure 5a, and can be expressed as follows:

$\tan(\theta/2) = (\Delta_1 / 2) / H$ ….. Eq. 001

where $\Delta 1$ is the total reduction in gap distance. Since θ is a small angle, the equation can be expressed as

$\theta = \Delta_1 / H$ ….. Eq. 002

where θ is measured in radians, and the range of Δ_1 has the limits [$\Delta 1 = 0 \rightarrow D_{gap}$].

When the displacement Δ_1 reaches the value of D_{gap} ,the 2 bumpers touch each other (figure 5b), and the value of θ at this point is denoted as θ_{limit} , and can be expressed as

$\theta_{limit} = D_{gap} / H$ ….. Eq. 003

Once the rotation exceeds the above limit (figure 5c), the air gap is already closed, and the joint movement is resisted by the stiffness of the rubber bumpers which are compressed, as the rotation increases.At this stage,

additional deformation at the top can be seen in figure 5c, where the total compressive deformation in the 2 bumpers is expressed as Δ_2 , and the rotation angle θ exceeds the value of θ_{limit}, and can be expressed as

$\tan(\theta/2) = [(\Delta_2 / 2) + (D_{gap} / 2)] / H$ ….. Eq. 004

Using small angle assumption,

$\theta = [\Delta_2 + D_{gap}] / H$ ….. Eq. 005

Simplifying, and substituting Eq.003 into Eq.005,

$\theta = \Delta_2 / H + \theta_{limit}$ ….. Eq. 006

and the elastic compressive deformation can be expressed as

$\Delta_2 = H (\theta - \theta_{limit})$ ….. Eq. 007

The relationship between the resulting compression force (P) at the top of the pontoons and the deformation in the rubber bumpers can be expressed using Hooke's law as

$P = [E A / (D_{bmp} /2)] * \Delta_2 / 2$ ….. Eq. 008

where

E is Young's modulusfor rubber (assumed as 7 MPa for this study).
A is the area of the bumper covering the top of the pontoon section.
D_{bmp} is the total thickness of the 2 bumpers together.

Since the tension force at the bottom joint is the same as the compression force developed at the top, the resulting bending moment (M) is simply the product of the compression force (P) and the height between the bottom and top joints (H). Substituting for (P) from Eq. 008, and for (Δ_2) from Eq. 007, the expression for the bending moment (M) which develops after the joint closes, can be expressed as

$M = PH = [E A H^2 / D_{bmp}] (\theta - \theta_{limit})$ ….. Eq. 009

In more general terms, the relation between the rotation angle at the joint and the developed bending moment can be expressed as :

$M = K_{ROT} (\theta - \theta_{limit}), \quad \theta > \theta_{limit}$

$M = 0, \quad \theta < \theta_{limit}$ ….. Eq. 010

Where the rotational stiffness of the joint (K_{ROT}) is expressed as

$K_{ROT} = E A H^2 / D_{bmp}$ ….. Eq. 011

The overall Moment-Rotation relationship of the newly developed joint can be illustrated in figure 6, where the different stages of its action are highlighted.

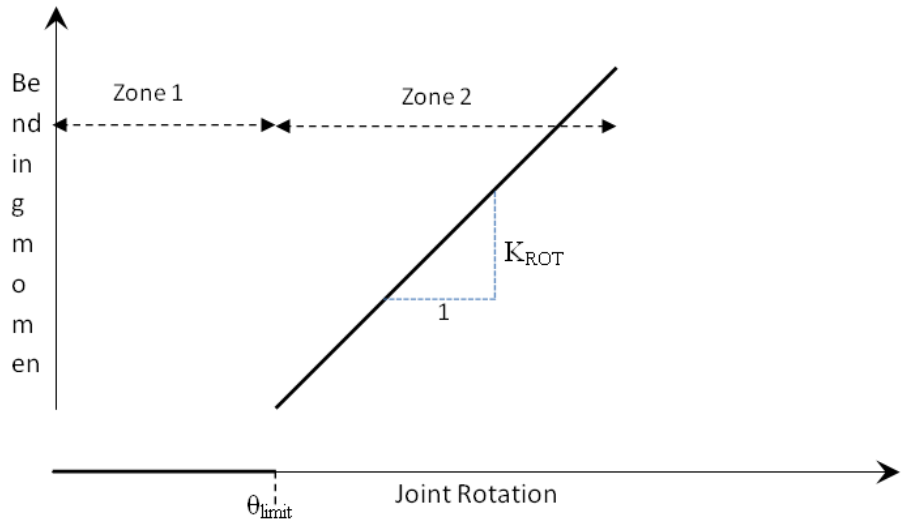

ANALYTICAL ALGORITHM

For ribbon type bridges, with hinges between them, the movements of the pontoons are very close to "rigid movements" with displacements and rotations at the edges. Neglecting the effect of internal deformations within the pontoons is therefore acceptable.

5.1. Development of pontoon-water thrust combined stiffness

For a single pontoon partially submerged in water, the upthrust force at any point is a function of the weight of the displaced fluid at this point, and thus is directly proportional to the pontoon bottom vertical displacement inside water at this point. This case is therefore, similar to the case of a beam on elastic

foundations. However, the elastic foundations in this case is the supporting fluid, and the supporting springs are the water upthrust forces.

As shown in Figure 7, the upward water stresses at nodes i & j at the 2 ends of the pontoon are defined as S_i&S_j , respectively.

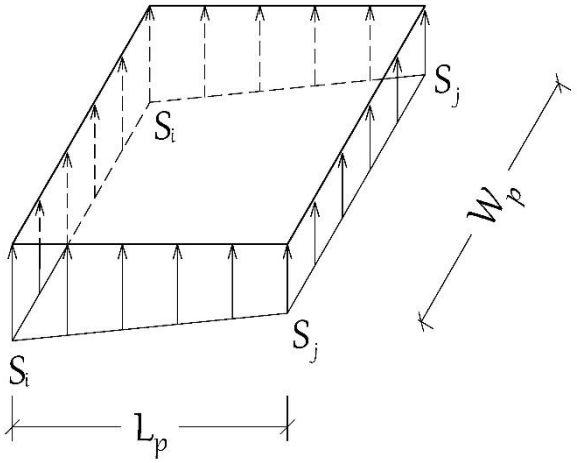

Figure 7. Water upthrust stress pattern on bridge pontoon.

The values of S_i& S_j can be expressed as:

$S_i = \gamma_{water} * y_i$,

$S_j = \gamma_{water} * y_j$, ….. Eq. 012

Where γ_{water} is the density of water (assumed as 1 t/cu.m).

And y_i& y_j are the submerged displacements of the pontoon bottom at points (i & j) respectively, under the water surface.

By summation of the stresses along the pontoon width (W_p), and dividing the stress pattern under the pontoon into 2 triangles as shown in figure 8a & 8b, the pontoon is idealized as a hinged-hinged beam element

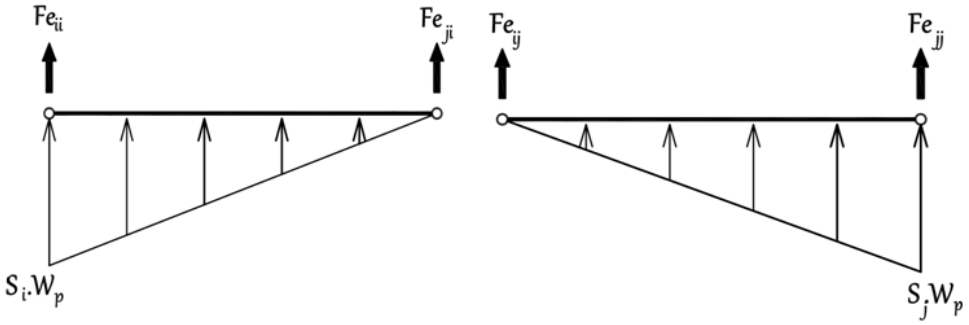

Figure 8. Idealization of water pressure and equivalent forces on single bridge pontoon

The equivalent forces (F_e) at the 2 nodes (i & j) can be computed as follows:

$F_{eii} = S_i \cdot W_p \cdot (L_p/2) \cdot (2/3) = \gamma_{water} * (W_p \cdot L_p/6) * (2) * y_i$

$F_{eji} = S_i \cdot W_p \cdot (L_p/2) \cdot (1/3) = \gamma_{water} * (W_p \cdot L_p/6) * (1) * y_i$

$F_{eij} = S_j \cdot W_p \cdot (L_p/2) \cdot (1/3) = \gamma_{water} * (W_p \cdot L_p/6) * (1) * y_j$

$F_{ejj} = S_j \cdot W_p \cdot (L_p/2) \cdot (2/3) = \gamma_{water} * (W_p \cdot L_p/6) * (2) * y_j$

….. Eq. 013

Adding the resulting equivalent forces at each of the 2 nodes, and putting the equations in matrix format, the relation between the nodal displacements and the nodal forces (total shear forces at the nodes) can be expressed as:

$$\begin{bmatrix} F_{i-j} \\ F_{j-i} \end{bmatrix} = \begin{bmatrix} F_{eii} + F_{eij} \\ F_{eji} + F_{ejj} \end{bmatrix} = \gamma_{water} \, (W_p \cdot L_p/6) \begin{bmatrix} 2 & 1 \\ 1 & 2 \end{bmatrix} \begin{bmatrix} y_i \\ y_j \end{bmatrix}$$ ….. Eq. 014

The above equation can be used as the stiffness equation relating end forces to end displacements of the element (including water support stiffness). It can be shortened as follows:

$\{F\} = [K]\ \{y\}$ ….. Eq. 015

Where [K] is the element stiffness matrix expressed as:

$$[K] = \begin{bmatrix} K_{ii} & K_{ij} \\ K_{ji} & K_{jj} \end{bmatrix} = \gamma_{water}\ (W_p\ .\ L_p\ /6)\ \begin{bmatrix} 2 & 1 \\ 1 & 2 \end{bmatrix} \text{ ….. Eq. 016}$$

And {F} & {y} are the force and displacement vectors at the pontoon ends.

Based on the local element stiffness matrix developed in Eq.016, a global stiffness matrix for a number of pontoons constituting part or whole of the bridge can be assembled to represent the stiffness of the bridge pontoons against movement into the underlying fluid, for the case of purely hinged connections taking into consideration the water support stiffness effect.

5.2. Nonlinear formulation of equilibrium equations of partial-fixation joint

Introducing the effect of partial fixation joints has the effect of changing the problem at hand from a linear to a nonlinear problem, where the stiffness matrix needs to be modified every time a joint closes ($\theta > \theta_{limit}$), thus requiring a nonlinear iterative approach to reach the final solution.Instead of modifying the global stiffness matrix several times during the analysis, a different nonlinear analysis approach is adopted here, through a combination of the virtual work method, and the stiffness method.

As the above stiffness equations are developed based on shear force-vertical displacement relations only for a rigid body pontoon, the effect of a bending moment developed at any hinged joint is translated into a couple acting on the 2 nodes of the element as shown in figure 9.

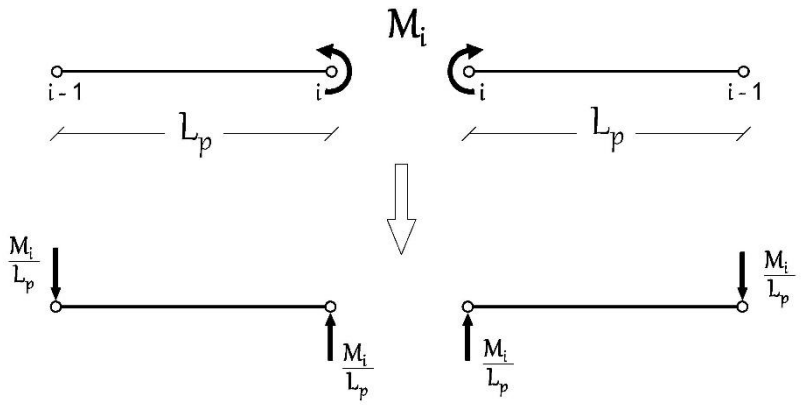

Figure 9. Equivalent nodal forces to a bending moment developed at partial-fixation joint

The equivalent nodal load vector for a bending moment acting at node (i), is composed of 3 forces acting at the specified node, and the 2 nodes surrounding it. The equivalent force vector can be expressed as follows:

$$\begin{bmatrix} F_{i-1} \\ F_i \\ F_{i+1} \end{bmatrix} = \begin{bmatrix} -M_i\ /\ L_P \\ +2\ M_i\ /\ L_P \\ -M_i\ /\ L_P \end{bmatrix} \text{ ….. Eq. 017}$$

Solving (Eq. 015) for a given set of wheel loads is a straightforward linear problem. This case will be refered to henceforth as CASE (0), as it constitutes the basic case of bridge analysis under vertical loads in the purely hinged case. The final displacement vector resulting from this analysis will be refered to as $\{\delta_0\}$. The corresponding relative rotations between the adjacent pontoons can be determined directly from the pontoons' displacements. Since fully rigid pontoon uints are assumed, the relative rotation at any joint (i) is the difference between the slopes of the 2 adjacent pontoons, and can be expressed as follows:

$\alpha_i = (y_i - y_{i-1}) / L_p - (y_{i+1} - y_i) / L_p = [2\ y_i - y_{i+1} - y_{i-1}] / L_p$…..Eq. 018

The sign of the rotation angle is therefore positive, when $y_i$is larger than the average of (y_{i+1}& y_{i-1}). The resulting vector comprising the relative rotations between pontoons at all joints will be refered to as $\{\alpha_0\}$.

For the simple case of only ONE (partial-fixation) joint developing moments at any joint (n), the force vector can be computed using (Eq. 017), and the corresponding displacement vector $\{\delta_n\}$ can be determined by solving (Eq. 015) for this case of loading. The corresponding rotations vector can also be computed using (Eq. 018), and is refered to as $\{\alpha_n\}$.

The virtual work equation for computing the magnitude of the developed bending moment at this "partial-fixation" joint (n) is expressed as

$\alpha_{on} - M_n\alpha_{nn} = \theta_{limit} + M_n / K_{ROT}$ …..Eq. 019

Rearranging the equation to obtain the value of M_n,

$M_n = (\alpha_{on} - \theta_{limit}) / (\alpha_{nn} + 1 / K_{ROT})$ .....Eq. 020

It is to be noted that the above equations (019 & 020) only apply when the resulting rotation at joint (n) has exceeded the value of θ_{limit}. The nonlinearity of the problem is therefore addressed through a check on the magnitude of rotations at the joints, and applying the equation only at locations where the limited has been exceeded. For the case of multiple joints reaching rotation values above θ_{limit}, and developing "partial-fixation" moments, the virtual work equations are developed to take into effect the relative rotations produced by each developed bending moment on all bridge joints. An example of "partial-fixation" moments developing at 3 joints (q,r & s) is shown below.

$\alpha_{oq} - M_q\alpha_{qq} - M_r\alpha_{rq} - M_s\alpha_{sq} = \theta_{limit} + M_q / K_{ROT}$

$\alpha_{or} - M_q\alpha_{qr} - M_r\alpha_{rr} - M_s\alpha_{sr} = \theta_{limit} + M_r / K_{ROT}$

$\alpha_{os} - M_q\alpha_{qs} - M_r\alpha_{rs} - M_s\alpha_{ss} = \theta_{limit} + M_s / K_{ROT}$ .....Eq. 021

Where α_{rq} is the rotation developed at joint (q) by a unit moment acting at joint (r). All other rotations in the above equation are similarly expressed. For any number of joints developing "partial-fixation" moments, the above equations can be put in matrix form and solved to obtain the values of the developed bending moments at these joints.

Once the values of the bending moments are determined at all joints where the rotation exceed the value of θ_{limit}, the final displacement and rotation at any node (n) can be obtained as follows:

$\delta_{final\text{-}n} = \delta_{on} + M_q\delta_{qn} + M_r\delta_{rn} + M_s\delta_{sn}$.....Eq. 022

$\alpha_{final\text{-}n} = \alpha_{on} + M_q\alpha_{qn} + M_r\alpha_{rn} + M_s\alpha_{sn}$.....Eq. 023

These equations can be extended to include any number of "partial-fixation" joints, and can be used repeatedly to determine the final displacements and rotations at all pontoon joints ($\{\delta_{final}\}$ & $\{\alpha_{final}\}$)

5.3. Step by Step Procedure

Application of the above-mentioned combined (stiffness-virtual work) approach is achieved through the development of a software package using (Visual Basic on Excel). The package is based on the step by step procedure outlined in the following steps:

1. A number of pontoons is selected so as to be sufficient to describe the overall bridge behavior, and the acting loads, and their locations are fixed for the required case of loading.
2. The allowable air gap distance and rubber bumper stiffness are computed. The values of the allowable rotation (θ_{limit}), and the rotational stiffness of the joints (K_{ROT}) are computed, using Equations 003&011.
3. The overall stiffness matrix of the "fully-hinged pontoons" case is developed, using Eq. 016, and inverted to obtain $[K]^{-1}$.
4. The force vector for Case [0] is developed to include the applied vehicle load, in addition to the pontoon own weights. Equation 015 is used for analysis to obtain the values of the displacement $\{\delta_0\}$ & rotation $\{\alpha_0\}$ vectors.
5. Force vectors are developed for possible cases of moments developing at each joint, using Eq. 017, and applied into equation 015. Analysis is performed to develop the displacement and rotation vectors for each "partial-fixation" moment case.
6. Analysis results for Case [0] obtained in step 4, are checked to determine the number of joints where the resulting rotation exceeds the value of θ_{limit}.
7. If ONE or MORE joints show values of relative rotation exceeding θ_{limit}, the joint with the highest value of relative rotation is selected.
8. The developed bending moment at the selected joint is obtained using eq 020/021, and the final bridge displacements and relative rotationsbetween pontoons($\{\delta_{final}\}$ & $\{\alpha_{final}\}$) are computed using Eqs. 022 & 023.
9. The rotations vector computed in step 8 is checked again to determine the number of joints where the resulting rotation at a hinged joint between pontoonsstill exceeds the value of θ_{limit}.
10. If the number of joints determined in step 9 exceeds the number of joints selected for analysis in step 7, the next joint with the highest rotation value is added to the selected joints.
11. Steps 8 to 10 are repeated until the final rotations vector does not have any remaining joints where the rotation exceeds θ_{limit}. At this point, convergence of the nonlinear analysis is reached, and the final results are obtained.
12. The final displacements, and joint bending moment values are used to determine the final water upthrust force distribution, and the corresponding shear and moment values.

The above-described step by step procedure is applied into a software package, which utilizes the Visual Basic language linked to Excel sheets, and used for a wide range of analysis runs as described in the next sections.

V. Sample Analysis Of Pontoon Bridge With "Partial-Fixaton" Joints

In this section, a sample of the results obtained using the developed analytical algorithm and software package is presented. A number of spans were selected as an intermediate portion of the bridge, and analyzed for the same fixed parameters, for three cases, namely "hinge-jointed" bridge, "fix-jointed" bridge, and "partial-fix-jointed" bridge. The input parameters are listed in Table 1 below.

Bridge Pontoon Data		Vehicle loads	
Pontoon Length	7.0 m	Max. Total Load	90 tons
Pontoon Width	8.0 m	Number of wheels	3
Pontoon Height	1.2 m	Load/wheel	30 tons
Own weight of Pontoons	800 kg/m	Spacing between wheels	3 m

Table 1. Summary of the Data Used in the Analysis

The bridge data are based on actual existing under-capacity pontoons, while the vehicle loads are based on the current maximum load of 63 tons. Based on extensive analysis runs performed by **Qayed R. Eid (2016)**, an estimated dynamic amplification factor of 1.3 can be considered as a top value for the dynamic bridge displacements, and straining actions. An additional 10% is assumed to account for possible variations in vehicle loads, spacing between wheels, and other factors usually encountered in the field, reaching a final value of 90 tons maximum. The above data will be used as a base for all analysis runs in this section, and section 7.

Two main cases of loading are selected here based on location of loads relative to the bridge pontoon joints. Figure 10 shows the 2 cases of loading [I & II]. These 2 cases are selected as the cases where the maximum displacements and bending moments are expected to develop.

a. Case [I] – Vehicle load symmetrical around joint between pontoons

b. Case [II] – Vehicle load symmetrical around pontoon centerline

Figure 10. Selected cases of loading for maximum effect on pontoon bridge

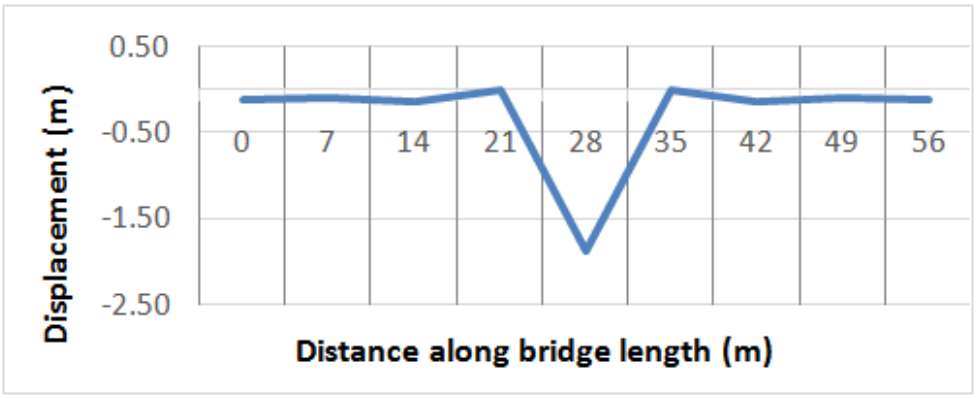

a. Vertical Displacement

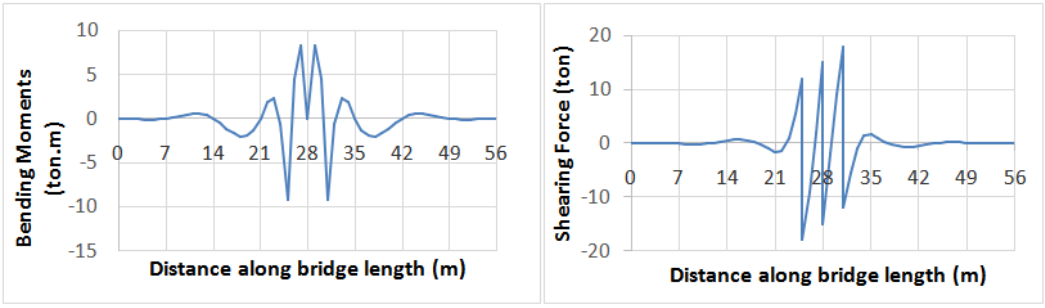

b. Bending Moments c. Shearing Forces

Figure 11. Analysis results for case of "Hinged-joint" pontoons bridge

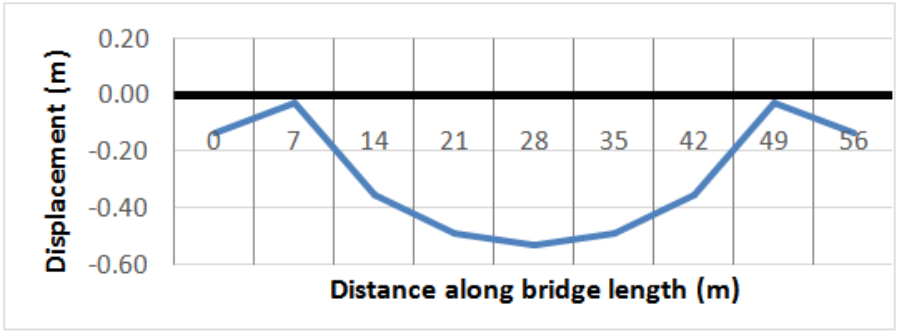

a. Vertical Displacement

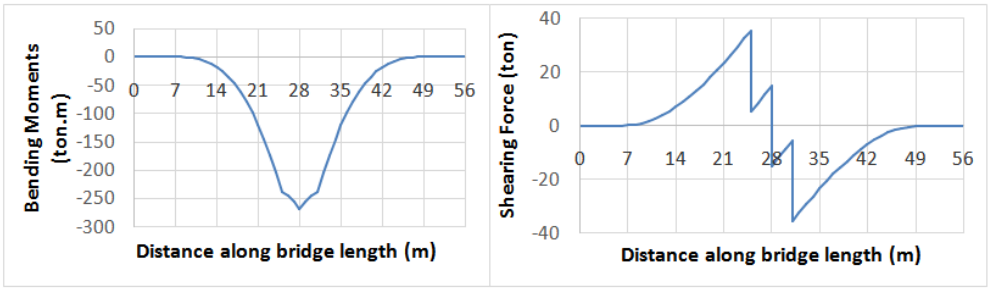

b. Bending Moments c. Shearing Forces

Figure 12. Analysis results for case of "Fixed-joint" pontoons bridge

Figure 11 shows the results obtained for the case of a totally hinged bridge, under total static and dynamic loads of 90 tons (Loading case [I]).The results show clearly that the pontoon sizes are not suitable to carry this high load. The vertical displacement of 1.88 m significantly exceeds the pontoon height, and therefore could lead to its drowning, and is definitely unacceptable. On the other hand, the bending moment values (in the +/- 10 mt range) is very small. This is the reason these existing pontoon units are not designed to have very strong longitudinal moment-resisting elements, and have been functioning successfully for years.

Figure12 shows the results obtained for the case of a totally fixed bridge, under total static and dynamic loads of 90 tons. This was achieved by reducing the air gap, and rubber thicknesses to near zero in the analysis, thus simulating conditions very near to total fixation. The results illustrate both the advantages and disadvantages of fixed joints. As can be seen, the vertical displacement has been reduced to a very small value (around 0.5 m), which is very safe for a 1.2 m height pontoon unit.

However, the huge increase in bending moment to a value of 268 mt poses a major problem, as the existing pontoons cannot withstand such high values of straining actions, and even attempts to strengthen these pontoons within the existing restraints may not be sufficient to reach such a high moment resisting capacity.

The value of (1.88 m) deflection for the hinged case, and (268 mt) bending moment for the fixed case will be used as datum throughout this discussion, for comparison of all results obtained using the partial-fixation proposed joints, in order to illustrate its effectiveness.

VI. Parametric Study

Analysis runs are performed while varying the gap distance D_{gap} from 1 to 20 cm, while at the same time varying the bumpers total width from 19 to 0 cm, so as to keep the total distance between pontoons always 20 cm. Two practical values for the bumper size were selected as (400 cm x 20 cm total)& (400 cm x 10 cm total), while Loading Case [I] is selected for all runs.Table 2 illustrates the input data for analysis run groups 1 to 6.

Analysis runs group Num.	Total Vehicle Load (tons)	Total Air Gap Size, D_{gap} (cm)	Rubber bumpers		
			Total width, D_{bmp} (cm)	Length (cm)	Height (cm)
1	70	1 to 20 (step of 1 cm)	19 to 0 (step of 1 cm)	400	20
2	80				
3	90				
4	70	1 to 20 (step of 1 cm)	19 to 0 (step of 1 cm)	400	10
5	80				
6	90				
7	90	1 to 20 (step of 1 cm)	Infinitely stiff steel bumpers		

Table 2. Input data for Analysis run groups 1 to 6

The analysis for run groups 1 to 3 are shown in figure 13. From the figure, it can be seen that increasing the air gap distance reduces the maximum bending moment value significantly. The rate of reduction is very high as the gap distance rises from 0 to 10 cm, and then slows down afterwards. The vertical displacement increases with the gap distance, but is in the rage of 0.8 to 1.0 m, throughout the whole interval.

This can be explained by the fact that in the first range of air gap distance (0 to 10 cm), the air gap closes very fast, and fixation moments develop early on. The closeness of the behavior in this range to that of a fixed bridge produces the shown high bending moment values. The increase in gap distance in this range produces a very fast drop in the maximum bending moment values, as the behavior moves towards "partial-fixation". In the range from about 10 cm to 20 cm air gap, the effect of the rubber bumper starts to appear, as the behavior does not change rapidly to a full-hinge behavior. No excessive downward deflection is noted, and the "partial-fixation" produces this notable slow change in both displacements and moments with the change in air gap distance.

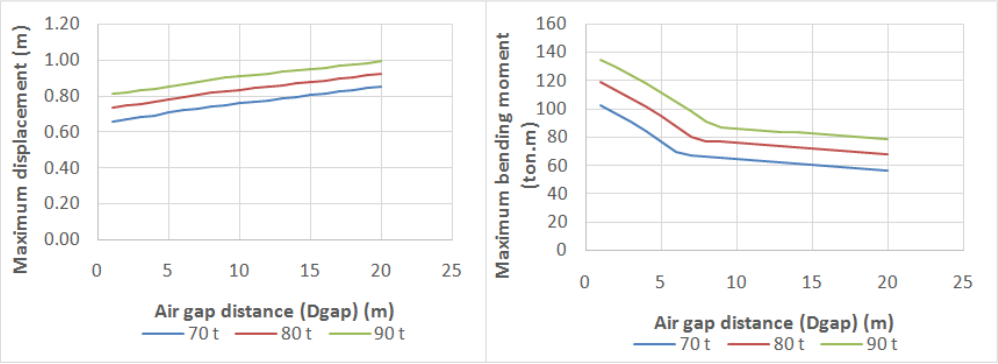

a. Maximum displacement b. Maximum bending moment

Figure 13. Variation of bridge maximum displacements and bending moments with air gap distance [Total distance between pontoon tops (D_{gap} +D_{bmp}) constant at 20 cm- bumper size (400 cm x 20 cm total)]

The analysis for run groups 4 to 6 are shown in figure 14. The results for these cases are similar to those obtained for run groups 1 to 3. However, it can be noted that the maximum bending moments for small gap sizes (1 to 5 cm) is much smaller than the corresponding values obtained in runs 1 to 3. This difference diminishes when reaching a gap size of 10 cm, and a bending moment value in the range of 80 to 90 mt is reached in both cases of runs 3 & 6.The deflections are higher but are still within the range of 0.9 to 1.0 for the 90 ton load. From the above results, the gap size of around 10 cm starts to appear as a reasonable value to be practically applied in developing the proposed partial-fixation joints.

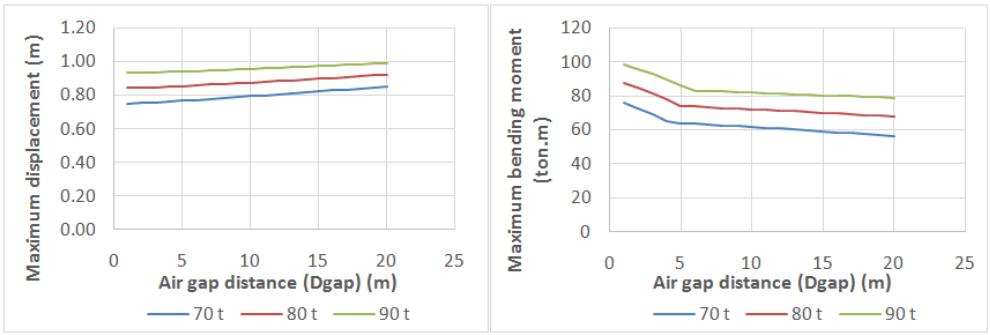

a. Maximum displacement b. Maximum bending moment

Figure 14. Variation of bridge maximum displacements and bending moments with air gap distance [Total distance between pontoon tops (D_{gap} +D_{bmp}) constant at 20 cm- bumper size (400 cm x 20 cm total)]

An additional group of runs (group 7) are performed on the bridge under the effect of a vehicle of total static and dynamic loads of 90 tons, while assuming steel bumpers. The steel bumpers are assumed to be infinitely stiff, and thus the joint rotation allowed by its deformation is neglected. The input data are listed in table 2, while figure 15 illustrates the results as compared to those of Analysis run groups 3 & 6.

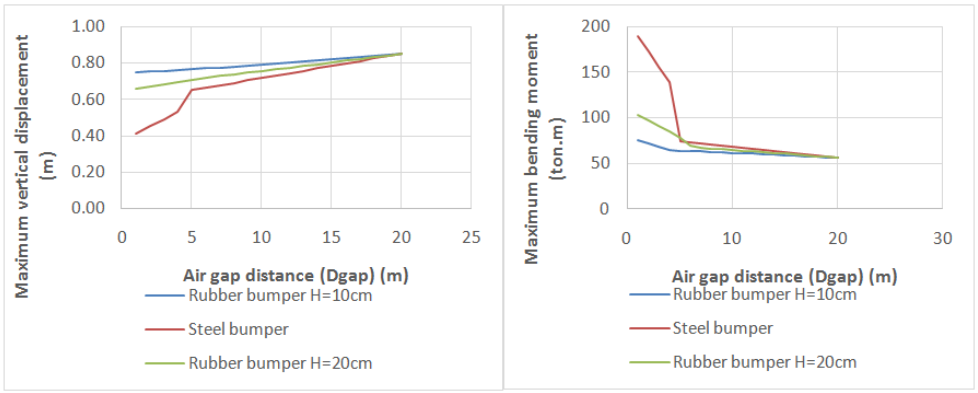

a. Maximum displacement b. Maximum bending moment

Figure 15. Comparison of pontoon bridge behavior for cases of "partial-fixation" joints fitted with steel vs rubber bumpers

It can be seen from figure 15b that the addition of rubber bumpers affects the results significantly for small values of air gaps as compared to the case of using steel bumpers. At a specific air gap value, the behavior of the joint starts to diverge for the 2 cases. This specific value is around 5 cm in the selected cases. As shown, as the air gap is reduced below this limit, the steel bumpers cause a rapid and sharp rise in bending moment values and a corresponding drop in displacement values, as compared to the case of rubber bumpers. This is caused by the added rotation allowed by the rubber bumper. In case of the steel bumper, for air gaps in the range from 0 to 5 cm, the joint is acting structurally very close to a fixed joint, thus the high moments and rapid variation. In the range of air gaps higher than 5 cm, the behavior of pontoons fitted with steel bumpers is very close to those fitted with rubber bumpers, although the maximum bending moment is still slightly higher.

The advantage of using rubber bumpers, as compared to using steel bumpers can be seen clearly in figure 15. The slow rate of change of the maximum deflection and bending moments with the change of air gap size in case of the rubber bumpers makes it highly recommendable, as no sudden rise in bending moments is to be expected. Taking into consideration the fact that the air gaps between the bumpers can be affected by other loads such as transverse current loads, this is highly desirable in order to avoid possible damage to the pontoons or the joints in case of a sudden rise in straining actions. It can also be seen that the less stiff rubber bumper (H=10cm) gives better results as the maximum bending moment obtained for analysis runs group 3 is less than that of group 6. Accompanying the reduction in maximum bending moment, the results always show that an increase in maximum displacement is noted (Figure 15a). However, the maximum vertical displacements do not exceed 90 cm in all cases under the 90 ton (static + dynamic) vehicle load together with the bridge's own weight, which is normal and safe for the standard 120 cm height pontoons. Further reduction in the maximum displacement is not needed, as it would entail an increase in the maximum bending moment values.

VII. Practical Application

For existing bridges, the total gap distance (D_{total}) between the top points of the 2 pontoons is variable. In order to develop results of practical value for the strengthening process, a practical range of values for the air gap is assumed, and a specific value for it is kept constant for each Analysis run group as shown in Table 3. Values of the rubber bumpers total width in the range of 5 to 15 cm are also used in each group of analysis runs.

Analysis runs group Num.	Total Air Gap Size (cm)	Total rubber bumpers width (cm)
8	5	5 / 7.5 / 10 / 12.5 / 15
9	7.5	5 / 7.5 / 10 / 12.5 / 15
10	10	5 / 7.5 / 10 / 12.5 / 15
11	12.5	5 / 7.5 / 10 / 12.5 / 15
12	15	5 / 7.5 / 10 / 12.5 / 15

Table 3. Input data for Analysis run groups 7 to 11

Analysis run groups (8, 9, 10 , 11 & 12) are performed with the purpose of providing designers with "design tables and curves" for the standard 7 x 8 x 1.2 m pontoon bridge. Table 3 shows the input data for the 5 groups of analysis runs, while the main results are summarized in Tables 4 to 6, for loading cases [I], [II], and envelope of [I & II], respectively. Figure 16 shows the variation of the expected maximum bending moments envelopes and maximum vertical displacements envelopes (Cases [I & II]), with the rubber bumper total width, for different values of air gap widths.

D_{gap} (cm)		5	7.5	10	12.5	15
D_{bmp} (cm)	K_{bmp} (t/cm)					
5	56.00	126.4	100.2	86.2	83.4	80.5
6	46.67	120.0	95.6	85.4	82.5	79.7
7	40.00	114.4	91.7	84.5	81.7	78.9
8	35.00	109.5	88.1	83.7	80.9	78.2
9	31.11	105.1	85.6	82.9	80.1	77.4
10	28.00	101.2	84.8	82.1	79.4	76.7
11	25.45	97.7	84.0	81.3	78.6	75.9
12	23.33	94.5	83.2	80.5	77.9	75.2
13	21.54	91.6	82.4	79.8	77.1	74.5
14	20.00	88.9	81.6	79.0	76.4	73.8
15	18.67	86.5	80.9	78.3	75.7	73.1

a. Maximum bending moments

Dgap (cm)		5	7.5	10	12.5	15
Dbmp (cm)	Kbmp (t/cm)					
5	56.00	0.805	0.864	0.909	0.941	0.973
6	46.67	0.825	0.879	0.919	0.950	0.982
7	40.00	0.842	0.893	0.928	0.959	0.991
8	35.00	0.858	0.905	0.938	0.968	0.999
9	31.11	0.873	0.916	0.947	0.977	1.008
10	28.00	0.886	0.925	0.956	0.986	1.016
11	25.45	0.898	0.934	0.964	0.994	1.024
12	23.33	0.910	0.943	0.973	1.003	1.032
13	21.54	0.920	0.952	0.981	1.011	1.040
14	20.00	0.930	0.961	0.990	1.019	1.048
15	18.67	0.940	0.969	0.998	1.027	1.056

b. Maximum displacement

Table 4. Maximum displacements and moments along bridge length – Loading Case [I]

Dgap (cm)		5	7.5	10	12.5	15
Dbmp (cm)	Kbmp (t/cm)					
5	56.00	132.1	120.4	108.8	97.1	85.4
6	46.67	128.3	117.0	105.7	94.4	83.1
7	40.00	124.7	113.8	102.8	91.9	81.0
8	35.00	121.3	110.7	100.2	89.6	79.0
9	31.11	118.2	107.9	97.6	87.4	77.1
10	28.00	115.2	105.2	95.3	85.3	75.4
11	25.45	112.4	102.7	93.0	83.4	73.7
12	23.33	109.7	100.3	90.9	81.5	72.1
13	21.54	107.2	98.1	88.9	79.8	70.7
14	20.00	104.8	95.9	87.1	78.2	69.3
15	18.67	102.6	93.9	85.3	76.6	67.9

a. Maximum bending moments

Dgap (cm)		5	7.5	10	12.5	15
Dbmp (cm)	Kbmp (t/cm)					
5	56.00	0.728	0.768	0.807	0.847	0.887
6	46.67	0.741	0.779	0.818	0.856	0.895
7	40.00	0.753	0.790	0.828	0.865	0.902
8	35.00	0.765	0.801	0.837	0.873	0.909
9	31.11	0.775	0.810	0.845	0.880	0.915
10	28.00	0.786	0.820	0.854	0.888	0.922
11	25.45	0.795	0.828	0.861	0.894	0.927
12	23.33	0.804	0.836	0.868	0.900	0.933
13	21.54	0.813	0.844	0.875	0.906	0.938
14	20.00	0.821	0.851	0.882	0.912	0.942
15	18.67	0.829	0.858	0.888	0.917	0.947

b. Maximum displacement

Table 5. Maximum displacements and moments along bridge length – Loading Case [II]

Dgap (cm)		5	7.5	10	12.5	15
Dbmp (cm)	Kbmp (t/cm)					
5	56.00	132.1	120.4	108.8	97.1	85.4
6	46.67	128.3	117.0	105.7	94.4	83.1
7	40.00	124.7	113.8	102.8	91.9	81.0
8	35.00	121.3	110.7	100.2	89.6	79.0
9	31.11	118.2	107.9	97.6	87.4	77.4
10	28.00	115.2	105.2	95.3	85.3	76.7
11	25.45	112.4	102.7	93.0	83.4	75.9
12	23.33	109.7	100.3	90.9	81.5	75.2
13	21.54	107.2	98.1	88.9	79.8	74.5
14	20.00	104.8	95.9	87.1	78.2	73.8
15	18.67	102.6	93.9	85.3	76.6	73.1

a. Maximum bending moments envelope

Dgap (cm)		5	7.5	10	12.5	15
Dbmp (cm)	Kbmp (t/cm)					
5	56.00	0.805	0.864	0.909	0.941	0.973
6	46.67	0.825	0.879	0.919	0.950	0.982
7	40.00	0.842	0.893	0.928	0.959	0.991
8	35.00	0.858	0.905	0.938	0.968	0.999
9	31.11	0.873	0.916	0.947	0.977	1.008
10	28.00	0.886	0.925	0.956	0.986	1.016
11	25.45	0.898	0.934	0.964	0.994	1.024
12	23.33	0.910	0.943	0.973	1.003	1.032
13	21.54	0.920	0.952	0.981	1.011	1.040
14	20.00	0.930	0.961	0.990	1.019	1.048
15	18.67	0.940	0.969	0.998	1.027	1.056

b. Maximum displacement envelope

Table 6. Maximum displacements and moments along bridge length – Envelope of Loading Cases [I & II]

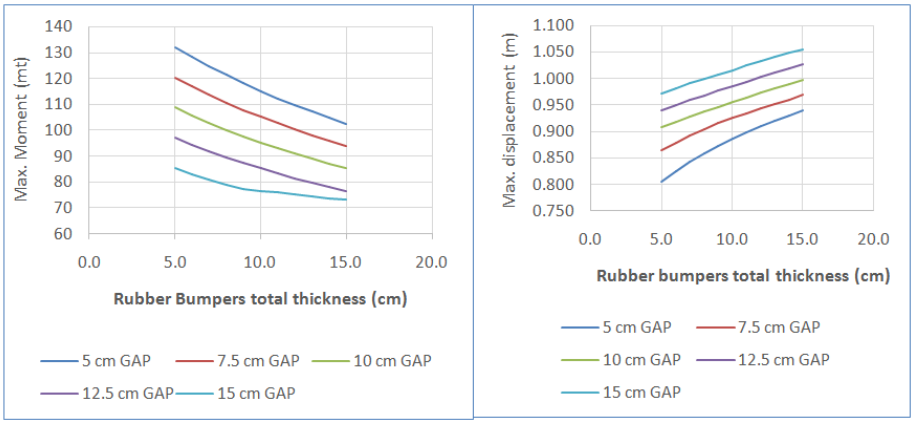

a. Maximum bending moment b. Maximum vertical displacements envelope

Figure 16. Variation of Maximum displacements and moments envelopes [Cases I & II] along bridge length with Air Gap and Rubber Bumper Sizes

Comparing Tables 4 & 5 results, it is clear that the maximum displacement is almost invariably obtained from Case [I] loading, while the maximum moments are obtained sometimes from Case [I], and sometimes from Case [II] loading. The envelope of maximum values obtained form both cases is presented in Table 6, and figure 16.

The final analysis results envelopes shown in Table 6 and figure 16 provide a useful tool for designers. For the standard 7 x 8 x 1.2 m pontoon bridge, the developed design curves and tables can be used for the assessment of the expected displacements and straining actions in case of using "partial-fixation" joints. Values of the bumper stiffness were listed in the tables in order to allow for its use in case the designer uses rubber bumpers with different values for Young's modulus, and varying dimensions. The designer can easily propose reasonable values for dgap and dgap , based on the actual separation distance between pontoon tops in the bridges under study, and use the curves to reach acceptable values of displacement and bending moment based on the estimated strength of the specific pontoons he is using.

VIII. Conclusions

- The newly proposed "partial-fixation" joint is studied in detail in this research, and is found to be an excellent tool for reduction of the maximum vertical displacements of ribbon type floating bridges, thus increasing the bridges' capacity for carrying higher loads.
- The flexibility of the rubber bumpers used in the proposed joint was found to be highly effective in controlling the levels of straining actions developed in the bridge body.
- At suitable configurations of use of the "partial-fixation" joints for standard 7 x 8 m pontoons, the expected maximum bending moments along the bridge length were found to be highly reduced as compared to the maximum bending moments expected in case of "full-fixation" bridges. This is an excellent advantage, as it allows for use of the existing pontoons with "Minimum or No" internal strengthening.
- The analytical algorithm and software package developed for the nonlinear analysis of pontoon bridges, fitted with the proposed "partial-fixation" joints has the advantage of being highly efficient, with a very short computer run-time, and provides the user with results in a form that is very easy to monitor. The software determines accurately which joints will reach the partial-fixation limit, and start to develop bending moments, and which joints will not reach the limit. The software results include final bridge displacements, and longitudinal shear and moments, displayed in graphs.
- The proposed joint was found to have an excellent effect on bridge behavior. The ability to control the gap distance between the joint's upper level bumpers makes it possible to exert excellent control on the expected bridge displacements and straining actions.
- In general, the effect of the proposed joint was found to reduce the pontoon displacements to acceptable limits, where the submerged height of the pontoon is reduced leaving sufficient height above water, thus providing adequate safety against excessive submerging, and against water reaching the passing vehicles, while keeping the straining actions developed within controllable limits.
- The increase in joint bumper-gap distance was found to reduce the level of fixation between pontoons, and therefore reduce the shear and bending moments resulting in the pontoons. The pontoons' displacements increase with increase of gap distance, but can still be controlled into acceptable downward displacement levels.
- The increase in vehicle weight passing on the bridge was found to increase the pontoon displacements, and internal shear forces and bending moments. However, analysis results showed that for the expected practical vehicle weight range, it is possible to determine a suitable joint configuration which reduces the downward displacement to acceptable limits without producing excessively high straining actions inside the pontoons.
- Design curves and tables were developed for use by design engineers for assessment of the expected displacements and straining actions in case of using "partial-fixation" joints. The curves were prepared for the standard 7 x 8 x 1.2 m pontoon bridge. However, similar curves can be prepared for bridges of different pontoon dimensions using the same algorithm and software package.

References

[1]. Wael M. Al-Badrawy, (2002) "Static and dynamic response of short span roadway bridge", M.Sc., Faculty of Engineering, Ain Shams University.
[2]. Shixiao Fu, Weicheng Cui, Xujun Chen and Cong Wang, (2005), "Hydroelastic analysis of a nonlinearly connected floating bridge subjected to moving loads " Marine Structures vol. 18 , 85-107.
[3]. Ehab M. Ebaied, (2006) "Analysis and design of floating bridges", PhD, Faculty of Engineering, Ain Shams University.
[4]. Shixiao Fu, Torgeir Moan, Xujun Chen and Weicheng Cui, (2007), "Hydroelastic analysis of flexible floating interconnected structures" Ocean Engineering vol. 34, 1516-1531.
[5]. Hisham A. El-Arabaty,(2007), "Analysis of floating bridges under transverse current loading" Scientific journal of civil engineering , faculty of engineering , Alazhar university,January 2007.

[6]. Mitra S. and Sinhamahapatra K.P., (2008), " 2D simulation of fluid-structure interaction using finite element method " Finite Element in Analysis and Design vol. 45 , Issue 1, 52-59.
[7]. Wael M. Al-Badrawy, (2009) "Dynamic response of road way bridges subjected to simultaneous vibration of multiple vehicles", PhD, Faculty of Engineering, Ain Shams university, .
[8]. Nasr E.Nasr,(2009) "Static and dynamic response of floating bridges to eccentric vehicle loads", PhD, Faculty of Engineering, Ain Shams University.
[9]. Giannin viecili (2014) "transportation optimization of ribbon floating bridges analytical and experimental investigation " open civil engineering journal 2014.8.42-56
[10]. Kayed R. Eid, (2016) "Strengthening of pontoons of ribbon type floating bridges", PhD, Faculty of Engineering, Ain Shams University.

Hisham A. El-Arabaty. "A Novel Proposal of Partial Fixation Joints to Raise The Load Carrying Capacity of Existing Ribbon Type Floating Bridges." IOSR Journal of Mechanical and Civil Engineering (IOSR-JMCE), vol. 16, no. 3, 2019, pp. 50-66